Brain circuitries in control of feeding behaviors

Focus on Neuropeptide Y

Gumbs, M.C.R.

Chapter VIII.
Afferent Neuropeptide Y projections to the ventral tegmental area in normal-weight male Wistar rats

Myrtille C.R. Gumbs, Anna H. Vuuregge, Leslie Eggels, Unga A. Unmehopa, Khalid Lamuadni, Joram D. Mul, and Susanne E. la Fleur

Journal of Comparative Neurology, 527(16): 2659-2674 (2019)

Abstract

The hypothalamic neuropeptide Y (NPY) circuitry is a key regulator of feeding behavior. NPY also acts in the mesolimbic dopaminergic circuitry, where it can increase motivational aspects of feeding behavior through effects on dopamine output in the nucleus accumbens (NAc) and on neurotransmission in the ventral tegmental area (VTA). Endogenous NPY in the NAc originates from local interneurons and afferent projections from the hypothalamic arcuate nucleus (Arc). However, the origin of endogenous NPY in the VTA is unknown. We determined, in normal-weight male Wistar rats, if the source of VTA NPY is local, and/or whether it is derived from VTA-projecting neurons.

Immunocytochemistry, *in situ* hybridization and RT-qPCR were utilized, when appropriate in combination with colchicine treatment or 24 hours of fasting, to assess NPY/*Npy* expression locally in the VTA. Retrograde tracing using cholera toxin beta (CTB) in the VTA, fluorescent immunocytochemistry and confocal microscopy were used to determine NPY-immunoreactive afferents to the VTA. NPY in the VTA was observed in fibers, but not following colchicine pretreatment. No NPY- or *Npy*-expressing cell bodies were observed in the VTA. Fasting for 24 hours, which increased *Npy* expression in the Arc, failed to induce *Npy* expression in the VTA. Double labeling with CTB and NPY was observed in the Arc and in the ventrolateral medulla.

Thus, VTA NPY originates from the hypothalamic Arc and the ventrolateral medulla of the brainstem in normal-weight male Wistar rats. These afferent connections link hypothalamic and brainstem processing of physiologic state to VTA-driven motivational behavior.

Introduction

Neuropeptide Y (NPY) is one of the most potent orexigenic peptides. Hypothalamic arcuate nucleus (Arc) NPY neurons and their projections throughout other regions of the hypothalamus have received substantial attention with regards to the role of NPY in feeding behavior (Clark et al., 1985; R. E. Mercer et al., 2011; Stanley, Chin, et al., 1985). However, it is now recognized that NPY interacts with the reward-related brain circuitry to regulate motivational aspects of feeding behavior (Liu & Borgland, 2015; Pandit et al., 2013; Quarta & Smolders, 2014). For example, administration of NPY into the lateral ventricle of rats increases motivation to obtain food pellets (Jewett et al., 1995). The ventral tegmental area (VTA) and nucleus accumbens (NAc) are important components of the reward-related brain circuitry in mediating feeding-related motivational behavior (Hernandez & Hoebel, 1988; Meye & Adan, 2014; Wise, 2004). We have previously demonstrated that NPY infusion specifically into the VTA or NAc, but not in the hypothalamus, increases the motivation to work for sugar without affecting intake of freely available sugar (Pandit et al., 2014a). In line with the effects of NPY on motivation, intracerebral- and intra-NAc NPY infusions increase dopamine concentrations in the NAc (Quarta et al., 2011; Sorensen et al., 2009). NPY also directly affects VTA dopaminergic neurotransmission via multiple pre- and postsynaptic mechanisms (Korotkova et al., 2006; K. S. West & Roseberry, 2017).

The effects of NPY on motivational behavior or mesolimbic neurotransmission have, however, been studied by applying exogenous NPY in the brain, and to date, no studies have investigated the role of endogenous NPY in these effects. The presence of NPY1 and NPY5 receptors (NPY1R, NPY5R) in the NAc and VTA indicates that endogenous NPY can interact with the reward-related brain circuitry (Korotkova et al., 2006; R. M. Parker & Herzog, 1999). For the NAc, the origin of endogenous NPY is both local as well as from an afferent Arc projection (Chronwall et al., 1985; de Quidt & Emson, 1986a; van den Heuvel et al., 2015). In contrast, the origin of endogenous NPY in the VTA is currently unknown. Studies on NPY-like immunoreactivity have demonstrated inconsistent results, reporting either the presence or absence of NPY-like immunoreactive cell bodies in the VTA (Chronwall et al., 1985; de Quidt & Emson, 1986a; Everitt et al., 1984). Furthermore, no studies to date have directly analyzed VTA NPY afferent projections using a neuroanatomical tracing approach. Endogenous NPY in the VTA could thus originate from local VTA interneurons, from afferent projections, or from both.

The aim of this study was to determine the source of endogenous NPY in the VTA. In addition, we investigated whether local VTA *Npy* expression is influenced by the physiologic state of the animal. Many NPY neurons in the brain present neuroanatomical features of interneurons (de Quidt & Emson, 1986a). Therefore, we hypothesized that the VTA would contain NPY-expressing interneurons. In addition, we hypothesized that the Arc and several

brainstem nuclei would contain NPY-positive projections to the VTA, as these brain areas are known to contain NPY-immunoreactive neurons as well as to project to the VTA (Chronwall et al., 1985; de Quidt & Emson, 1986a; Geisler & Zahm, 2005; Yamazoe, Shiosaka, Emson, & Tohyama, 1985). We investigated local VTA NPY/*Npy* expression using immunocytochemistry and *in situ* hybridization in normal-weight male Wistar rats. The effect of physiologic state on VTA *Npy* expression was measured by real time qPCR (RT-qPCR) of VTA brain punches of 24 hour-fasted and non-fasted controls. Afferent NPY VTA projections were determined following infusion of the fluorescence-conjugated retrograde tracer cholera toxin-Beta (CTB) into the VTA, using fluorescent immunocytochemistry and confocal microscopy to visualize co-localization with NPY-immunoreactive neurons. We examined brain regions that have been described to contain NPY-expressing neurons as well as to project to the VTA. In addition, as not all Arc -> VTA projecting neurons showed NPY immunoreactivity, we also assessed whether these neurons co-localized with pro-opiomelanocortin (POMC), the other major neuronal population in the Arc (R. D. Cone, 2005). This is the first study to systematically investigate the nature of the neuroanatomical relationship between NPY and the VTA of the reward-related brain circuitry.

Experimental procedures

Animals

Male Wistar rats (Charles River breeding Laboratories, Sulzfeld, Germany), weighing 240-280 g at arrival, were habituated to a temperature- (21-23 ˚C) and light-controlled room (12:12h light/dark cycle, 07:00-19:00 lights on) of the animal facility of The Netherlands Institute of Neuroscience. Rats had *ad libitum* access to a container of a standard high-carbohydrate diet (Teklad global diet 2918; 24% protein, 58% carbohydrate, and 18% fat, 3.1 kcal/g, Envigo) and a bottle of tap water. The animal care committees of the Amsterdam UMC of the University of Amsterdam and The Netherlands Institute for Neuroscience approved all experiments according to Dutch legal ethical guidelines.

Fluorescent immunocytochemistry

Every other VTA slice was used from colchicine-infused rats from the retrograde tracing experiment in which the tracer injection was not apparent (N = 4; see Retrograde tracing section below for details), or naïve rats perfused with cold saline and 4% paraformaldehyde (PFA) after i.p. injected pentobarbital (N = 3). Brains were post-fixed for 24 hours in 4% PFA and cryoprotected in 30% sucrose/PBS, and subsequently frozen on dry ice and stored at -80 ˚C. Cryostat sections (35 µm) were kept at -20 ˚C in cryoprotectant (30%v/v glycerol, 30%v/v glyceraldehyde, 40%v/v 10xPBS). Arc slices were used as positive controls and tyrosine hydroxylase (TH) staining was used to visualize dopaminergic neurons in the VTA.

Free-floating sections were washed in Tris-buffered saline (TBS; 50 mM Tris-Cl, 150 mM NaCl; pH 7.6) and incubated with 1:1,000 rabbit anti-NPY [Niepke 26/11/1988, RRID: AB_2753189, Netherlands Institute for Neuroscience, (Buijs, 1989)] and 1:1,000 mouse anti-tyrosine hydroxylase (#MAB318, RRID: AB_2201528, EMD Millipore Corporation, Temecula) in supermix (0.15 M NaCl, 0.05 M Tris, 0.25%w/v gelatin, 0.5%v/v Triton X-100, pH 7.6 at RT) in a humidified chamber for 1 hour at RT and overnight at 4 ˚C. After TBS washes, sections were incubated for 1 hour at RT with 1:400 biotinylated goat anti-mouse IgG (H+L) (BA9200; Vector Laboratories, Burlingham) in supermix. After TBS washes, sections were incubated with 1:500 Alexa Fluor-647-Streptavidin (s32357, Invitrogen, Carlsbad) and 1:500 Alexa Fluor-488 donkey anti-rabbit IgG (H+L) (A21206, Invitrogen) in supermix for 1 hour at RT. After TBS washes, sections were rinsed in PBS and incubated with 1:150 Hoechst (Pure Blue nuclear staining dye 33342; Biorad Laboratories, Hercules) in 1xPBS for 15 min at RT. After TBS washing, sections were coverslipped with Mowiol (10%w/v (Mowiol 4-88; Calbiochem, Merck, Darmstadt, Germany) in 0.1 M Tris-HCL pH 8.5, 25%v/v glycerol) and stored in the dark at 4 ˚C.

Procedures for immunocytochemistry for POMC are similar to those described for NPY staining. Briefly, slices were used from brains with tracer infused into the VTA (N = 6; same animals as for NPY retrograde tracing). In chronological order, antibodies for the different incubation steps were; 1:8,000 rabbit anti-POMC antibody (Lot. 01643-3, Cat# H-029-030, RRID: AB_2307442, Phoenix Pharmaceuticals, CA), 1:400 biotinylated anti-rabbit IgG (H+L) (BA1000; Vector Laboratories, Burlingham), 1:500 Alexa Fluor-647-Streptavidin (s32357, Invitrogen, Carlsbad), and 1:150 Hoechst (Pure Blue nuclear staining dye 33342; Biorad Laboratories, Hercules). Sections were stored as mentioned above.

Fluorescent *in situ* hybridization

After 7 days in the animal facility, naïve animals were sacrificed by decapitation after 30%CO_2/70%O_2 anesthesia for tissue collection (N = 6). Brains were rapidly dissected, frozen on dry ice and stored at -80 ˚C. Cryostat sections (35 µm) of the Arc and VTA were mounted, air-dried (40 min at 37 ˚C), and stored at -80 ˚C.

Tissue, materials and solutions were kept in RNAse-free conditions until after the stringency washes (see below). Arc sections and every other VTA section was defrosted and fixed in 4%w/v PFA in PBS (20 min at 4 ˚C). Sections were then pretreated with 0.25%v/v acetic anhydride in 0.1 M triethanolamine, washed in PBS and delipidated with 0.1% Triton X-100/PBS (10 min). After a PBS and a 1x standard saline citrate solution (SSC) wash, sections were pre-hybridized for 1 hour in hybridization buffer (HB) containing 50%v/v formamide, 600 mM NaCl, 10 mM HEPES Buffer (pH 7.5), 5xDenhardt's solution, 1 mM EDTA and 200 µg/mL denatured herring sperm DNA in Ultra-pure water. Sections were hybridized overnight with HB containing 3,000 ng/mL denatured antisense NPY RNA probe (Larhammar, Ericsson, & Persson, 1987) in a humidified chamber at 55 ˚C. Sequential stringency washes included;

5xSSC (5 min, 55 ˚C), 2xSSC (1 min, 55 ˚C), 0.2x SSC/50%v/v formamide (30 min, 55 ˚C), and 0.2xSSC (5 min, RT). Immunological detection ensued with 5 min washing in buffer 1 containing 100 mM Tris, 150 mM NaCl in Ultra-pure water (pH 7.5), 1 hour incubation with 1%w/v blocking reagent (11096176001, Roche Diagnostics, Mannheim Germany) in buffer 1, 5 min washing in buffer 1, and 3 hour incubation in 1:1,000 anti-DIG-alkaline phosphatase (11093274910, Roche Diagnostics, Mannheim, Germany) in buffer 1. After washing (buffer 1; 2x 15 min; buffer 2; 100 mM Tris, 100 mM NaCl, 5 mM $MgCl_2$, in Ultra-pure water, pH 9.5; 1x 5 min), sections were developed by overnight incubation with NBT/BCIP coloring solution (337.5 µg/mL nitroblue tetrazolium, 175.4 µg/mL 5-bromo-4-chloro-3-indolyl phosphate *p*-toluidine salt, 240 µg/mL levimasole in buffer 2). After sequential washing (distilled water, 100% methanol, distilled water; 5 min), sections were prepared for TH detection. All following incubations were separated by TBS washes. Sections were incubated in 1:1,000 mouse anti-TH in supermix in a humidified chamber for 1 hour at RT and overnight at 4 ˚C, for 1 hour in 1:400 biotinylated goat anti-mouse IgG (H+L) in supermix, and with 1:800/1:800 avidin/biotin complex (PK-6100, Vector Laboratories, Burlingham) in supermix for 1 hour at RT. Sections were developed with a Vector Red kit (SK-5100, Vector Laboratories, Burlingham), coverslipped, and stored as mentioned above. Arc sections were used as a positive control. As previously tested with this NPY probe (van den Heuvel, Eggels, Fliers, et al., 2014), no staining was seen in negative controls of VTA and Arc slices incubated without NPY probe.

<u>The effect of metabolic state on VTA *Npy* mRNA levels</u>

After 7 days in the animal facility, naïve rats were fasted for 24 hours (10:00–10:00) or kept under *ad libitum* conditions (N = 8 per group), and decapitated after 33%CO_2/66%O_2 anesthesia. Brains were rapidly dissected, frozen on dry ice and stored at -80 ˚C.

Sections (250 µm) were cut on the cryostat to obtain punches of the Arc (Bregma -1.72 till -3.48 mm) and bilaterally of the VTA (Bregma -4.68 till -6.24 mm [Paxinos & Watson, 2007]). Sections were placed in RNAlater (Ambion, Waltham, MA) and punched with a 1 mm-diameter blunt needle. Punches were stored in 300 µL (Arc) or 500 µL (VTA) TriReagent. After homogenization using an Ultra Turrax homogenizer (IKA, Staufen, Germany), total RNA was isolated by chloroform extraction followed by RNA purification using the Machery Nagel nucleospin RNA clean-up kit. RNA quality was determined using Agilent RNA nano chips, using the manufacturer's kit and instructions, and was analyzed with a Bioanalyzer (Agilent, Santa Clara, USA). Only RIN values larger than 8.50 were included. cDNA synthesis was carried out using equal RNA input (124.44 ng; measured with Denovix DS11; Denovix, Wilmington) and the transcriptor first-strand cDNA synthesis kit with oligo d(T) primers (04897030001; Roche Molecular Biochemicals, Mannheim, Germany). Genomic DNA contamination was controlled for by cDNA synthesis reactions without reverse transcriptase.

Gene expression was measured using RT-qPCR with the SensiFAST SYBR no-rox kit (Bioline, London, UK) and Lightcycler® 480 (Roche Molecular Biochemicals); 2 µL cDNA was incubated in a final reaction volume of 10 µL reaction containing SensiFAST and 25 ng per primer (see Table 1 for primer sequences). PCR products were analyzed on a DNA agarose gel for qPCR product size.

Table 1. List of primers for RT-qPCR.

Gene	NCBI ref. number	Forward primer 5'- 3'	Reverse primer 5'- 3'
Npy	NM_012614.2	GACAATCCGGGCGAGGACGC	TCAAGCCTTGTTCTGGGGGCA
Npy1r	NM_001113357.1	TCTCATCGCTGTGGAACGTC	CCGCCAGTACCCAAATGACA
Npy5r	NM_012869.1	GCCGAAGCATAAGCTGTGGAT	TTTTCTGGAACGGCTAGGTGC
Ubiq-C	NM_017314.1	TCGTACCTTTCTCACCACAGTATCTAG	GAAAACTAAGACACCTCCCCATCA
HPRT	NM_012583.2	CCATCACATTGTGGCCCTCT	TATGTCCCCCGTTGACTGGT
Cyclo-A	NM_017101.1	TGTTCTTCGACATCACGGCT	CGTAGATGGACTTGCCACC

Cyclo-A = Cyclophilin-A, *HPRT* = Hypoxanthine guanine phosphoribosyl transferase, *Npy1r* = Neuropeptide Y receptor subtype 1, *Npy5r* = Neuropeptide Y receptor subtype 5, *Npy* = Neuropeptide Y, *Ubic-c* = Ubiquitin-C

Retrograde tracing from the ventral tegmental area

After 7 days in the animal facility, rats (N = 22) were implanted with two cannulas; in the right VTA for the infusion of the retrograde tracer CTB conjugated to Alexa-555 (C-22843, Invitrogen, Bleiswijk, The Netherlands), and in the left lateral ventricle (LV) for the infusion of colchicine to block neuronal transport, which is required to visualize NPY cell bodies in the medial basal hypothalamus (de Quidt & Emson, 1986a). Stereotactic surgeries and infusions were performed as described previously (van den Heuvel, Eggels, Fliers, et al., 2014). Rats were anesthetized with a mix of ketamine (80 mg/kg; Eurovet Animal Health, Bladel, The Netherlands), xylazine (8 mg/kg; Bayer Health Care, Mijdrecht, The Netherlands) and atropine (0.1 mg/kg; Pharmachemie B.V., Haarlem, The Netherlands) intraperitoneally and fixed in a stereotactic frame. Lidocaine (AstraZeneca) was used for local analgesia of the periost. Permanent stainless steel guide cannulas were placed in the VTA (26 gauge; PlasticsOne, Bilaney Consultants GmbH, Düsseldorf, Germany) and LV (22 gauge) with coordinates A/P: -5.40 mm from Bregma, L: +2.4 mm, and V: -8.1 mm below the surface of the skull in an angle of 10° in the frontal plane, and A/P: -0.8 mm, L: +1.8 mm, and V: 4.0 mm below the surface of the brain, respectively. Cannulas were secured to the skull using three anchor screws and dental cement. Cannula's were occluded by stainless steel dummy cannula's. Immediately after surgery, rats received an analgesic subcutaneously (Carprofen, 0.5 mg/100 g body weight) and were housed individually for the rest of the experiment.

Directly after surgery and using pressure injection (Yi et al., 2006), 50-100 nL 1% CTB-Alexa555 was infused into the VTA at an infusion rate of 0.3 µL/min using a syringe infusion pump (Harvard apparatus) with a 10 µL Hamilton syringe connected to an injector (33 gauge, PlasticsOne) that extended 1 mm below the guide cannula. Ten days later, rats were anesthetized with pentobarbital and 100 µg colchicine (C9754, Sigma-Aldrich, Zwijndrecht, The Netherlands) in 5 µL 0.9% NaCL was infused in the LV at 10:00. Colchicine was infused at a rate of 1 µL/min. Both injections were confirmed by monitoring fluid movement in the tubing via a small air bubble. After completion of the infusion, the injector was left in place for 20 min to allow for diffusion and then replaced with dummy cannulas. Thirty hours after colchicine infusion, rats were deeply anesthetized with an i.p. injection of pentobarbital and perfused transcardially with cold saline followed by 4% PFA in 0.1 mol/L PBS (pH 7.6; 4 °C). Brains were removed and, after 24 hours postfixation, cryoprotected in 30% sucrose in PBS at 4 ˚C. Brains were frozen on dry ice and stored at -80 ˚C.

A cut was made in the cortex to allow determination of the ipsi- and contralateral side of the tracer infusion. Slicing, storing and staining procedures were performed as for fluorescent immunohistochemistry above. The injection site was determined in VTA slices counterstained with anti-tyrosine hydroxylase (1:1,000 rabbit anti-TH; T8700, Sigma,-Aldrich, Zwijndrecht, The Netherlands), biotinylated goat anti-rabbit IgG (H+L) (1:400, BA1000, Vector laboratories) and Alexa Fluor 647-Streptavidin (1:500, s32357, Invitrogen). Slices throughout the rostrocaudal length of the brain were stained for NPY as described above to determine co-localization with CTB (see below for details of the analysis). Slices were coverslipped and stored as written above for fluorescent immunocytochemistry.

Antibody characterization

All primary antibodies used in this study have been extensively characterized. The specificity of anti-NPY was tested by pre-absorption controls on human infundibular brain tissue (homologous to the rat Arc) and formalin-bound porcine NPY to nitrocellulose paper, as well as by testing for cross-reactivity with several peptides formalin-fixed onto gelatin-coated nitrocellulose paper (Buijs, 1989; Goldstone, Unmehopa, Bloom, & Swaab, 2002; van der Beek et al., 1992; van Wamelen, Aziz, Anink, Roos, & Swaab, 2013). The specificity of anti-POMC was tested by pre-absorption controls on Arc brain sections containing POMC neurons, where staining was abolished (Wittmann et al., 2017). The specificity of anti-TH was tested by Western Blot analysis of recombinant TH and of VTA protein homogenates, which showed that it recognized a single band of 56 – 60 kDa, and the absence of staining in midbrain-containing brain slices of animals in which dopamine neurons where specifically lesioned by 6-hydroxydopamine (H. L. Wang & Morales, 2008). We again confirmed the specificity of all primary and secondary antibodies by omitting the primary antibody in the staining procedure of Arc or VTA slices. This consistently resulted in complete absence of staining in the Arc or

VTA. We additionally used Western Blotting to confirm that the POMC antibody specifically recognizes a 29 kDa protein in Arc lysates from naïve male Wistar rats, and that the TH antibody specifically recognizes a 55-60 kDa protein in VTA lysates. Finally, the staining patterns of all primary antibodies are in accordance with previous studies that characterized NPY and POMC staining in the Arc, and TH staining in the VTA (H. L. Wang & Morales, 2008; Wittmann et al., 2017). See Table 2 on page 167 for a summary of the antibodies used in this study.

Microscopy and image analyses

VTA slices stained for *Npy* mRNA were analyzed by light microscopy using a Zeiss Axioskop 9801 with 2.5X (n.a. 0.075) and 10X (n.a. 0.30) PlanNeoPlan Fluar objectives (Zeiss) and a color camera (EvolutionMP; QImaging). Fluorescent stained slices were analyzed using widefield fluorescent microscopy on a Zeiss Axiovert 200M with Plan-NeoFluar objectives at 2.5X (n.a. 0.075) and 5X (n.a. 0.16) magnification to investigate local NPY peptide expression, VTA slices for infusion site determination for retrograde tracing, and for a quick scan for co-localization. Fluorescence was excited with a HXP 120 V power supply Metalhalide lamp with excitation filters 365/12 nM (Hoechst) 560/40 nM (Alexa Fluor 555), 470/40 nM (Alexa Fluor 488), and 605/50 nM (Alexa Fluor 647), and emission filters >397 nM, 603/75 nM, 515/30 nM, and 670/50 nM respectively. Images were obtained with a black and white camera (ExiAqua, QImaging) and ImageProPlus software (version 6.3, Media Cybernetics, USA). Co-localization was confirmed with confocal image series made with a Leica TCS SP8 X confocal microscope encompassing a Z-stack of the entire slice thickness and sequential excitation with a diode for Hoechst (450 nm), and a white light laser for CTB (555 nM) and NPY (647 nM). Hybrid detection settings were 415-460 nM, 565-605 nM, and 657-700 nM respectively. All images were taken with the same excitation and emission parameters. Image series were taken with 20X (n.a. 0.75) and 63X (n.a. 1.40) oil-immersion objectives with Immersol 518F (Zeiss) acquired at a digital resolution of 1024 x 1024 pixels in a unidirectional scan. Minimal Z-stack resolution was 2.50 µM.

For retrograde tracing, all LV cannulas were placed correctly as determined using thionine staining. Animals were included in retrograde tracing analysis when CTB and TH fluorescence overlapped with minimal CTB outside the TH-stained area or when the CTB fluorescent pattern was comparable to Geisler and Zahm (2005), using a similar approach to map all afferent projections to the VTA. Widefield fluorescent images were analyzed with ImageJ (Rasband, USA, http://rsbweb.nih.gov/ij/, 1997–2005) and confocal images with LAS AF Lite X (version 2.6.3, Leica microsystems). Every 10th slice was selected, stained and counted for the entire brain (Bregma 5.64 till -15.00 mm). For the Arc region (Bregma -1.08 till -4.68 mm) every 6th slice was sampled. Regions of interest were selected based on known VTA afferents from literature (Geisler & Zahm, 2005; Yetnikoff et al., 2014) and which express NPY

peptide. In widefield images for the investigation of co-localization, structures were delineated based on anatomical markers (visual anatomical structures such as ventricles or fiber tracts, and DAPI-staining) and NPY staining patterns. In regions where co-localization was detected, regions of interest were determined based on, and therefore always completely encompassed, the staining pattern of NPY or POMC in Z-stack confocal image series as those areas lack specific anatomical markers. Arc POMC neurons extend laterally into the peri-arcuate region, therefore POMC analysis included this area. For the brainstem region, this area was conform to the A1 and C1 catecholaminergic regions as described previously (Everitt et al., 1984; Harfstrand, Fuxe, Terenius, & Kalia, 1987; Sawchenko & Swanson, 1982). The Arc was thus contained in 11 sections at 210 µm intervals, and the brainstem area containing co-localization was contained in 8 sections at 350 µm intervals.

In structures determined to contain co-localization (by widefield image analysis and verification by confocal microscopy), the number of labelled neurons were counted in all sections that contained the structure according to the rat brain atlas (Paxinos & Watson, 2007). Structures were counted as cells if they contained a Hoechst-stained nucleus that was completely contained in the Z-stack, showed fluorescence at least 2x above background (executed by excluding signal intensity below 2x background, which was determined in slices incubated according to the staining protocol without primary antibody), and did not show an aberrant staining pattern (e.g. red or green fluorescence in the nucleus). The abundance of NPY cells in the Arc complicated their counting. Therefore, all CTB-containing cells within the NPY-regions were counted by scrolling through the Z-stack in the red and blue channel and labeling CTB neurons according to our criteria. Subsequently, co-localization was determined in recognized CTB cells by enabling the green channel within as well as next to the red channel. CTB-positive and CTB/NPY-positive neurons were counted ipsilateral and contralateral to the CTB infusion site. As all six rats showed a consistent number of CTB and CTB/NPY-positive neurons, the data are presented as the mean of the estimated total neuron number (N), calculated using the following equation: $N = \Sigma Q^{-} \cdot t/h \cdot 1/asf \cdot 1/ssf$, where ΣQ^{-} = total number of neurons counted per region, t = thickness of the section, h = height of the section, asf = areal sampling fraction, and ssf = section sampling fraction (M. J. West, Slomianka, & Gundersen, 1991). In our study t/h is equal to 1 as the entire section thickness was included, and 1/asf also equals 1 as the entire area of the region of interest was included. Therefore, the used formula equals to $N = \Sigma Q^{-} \cdot 1/ssf$ with ssf = 6 for the Arc and ssf = 10 for the brainstem. Subsequently, the percentage CTB-NPY/total CTB cells was calculated per hemisphere. In all other regions, confocal microscopy confirmed the absence of co-localization. Counts were performed independently by two investigators.

Statistics and analyses

RT-qPCR quantification was performed using LinReg Software (Ramakers et al., 2003). Samples deviating >5% from the mean PCR efficiency and outliers (Grubb's test) were excluded. Values were normalized using the geometric mean of three reference gene values (*Ubiquitin-C, Hypoxanthine guanine phosphoribosyl transferase and Cyclophilin-A*; see Table 1). All values were normalized to *ad libitum* controls. Compliance with normality and equal variance assumptions were confirmed with Shapiro-Wilk and Levene's test for equal variances respectively. Differences between groups were then evaluated using Two-way ANOVA analysis followed by the Bonferroni method for multiple comparisons (IBM SPSS version 24). All data are presented as mean ± *SEM*.

Results

Assessment of local NPY/*Npy* expression in the VTA

Many NPY-expressing neurons present anatomical characteristics representative of interneurons (de Quidt & Emson, 1986a). Therefore, we first determined whether the VTA contains NPY-immunoreactive cell bodies using fluorescent immunocytochemistry in brain slices containing the VTA (Figure 1a). NPY-immunoreactive fibers were found scattered throughout the VTA (Figures 1b-d, h). In contrast, no NPY-immunoreactive cell bodies were found throughout the full rostro-caudal extent of the VTA. Visualization of NPY can be enhanced by pre-treatment of animals with colchicine, which arrests neuronal peptide transport (Borisy & Taylor, 1967; de Quidt & Emson, 1986a). Consistent with the effects of colchicine on neuronal peptide transport, no NPY-immunoreactive fibers were found in the VTA (Figures 1e-g). Furthermore, colchicine treatment did not visualize NPY-immunoreactive cell bodies throughout the VTA. Collectively, these observations indicate that the NPY-immunoreactive fibers are part of an NPY afferent projection to the VTA.

We next used *in situ* hybridization to confirm the absence of NPY-expressing cell bodies in the VTA. Throughout the VTA, no *Npy*-expressing cell bodies were observed (Figures 2a-b). In contrast, *Npy*-expressing cell bodies were observed in the posterior lateral hypothalamic area and the medial supramammillary nucleus (Figures 2a-c), both located adjacent to the anterior VTA. As expected, positive control slices containing the Arc also showed strong expression of *Npy* in cell bodies (Figure 2d). Taken together, these findings indicate that NPY is not locally produced in the VTA, and that NPY afferents project to the VTA.

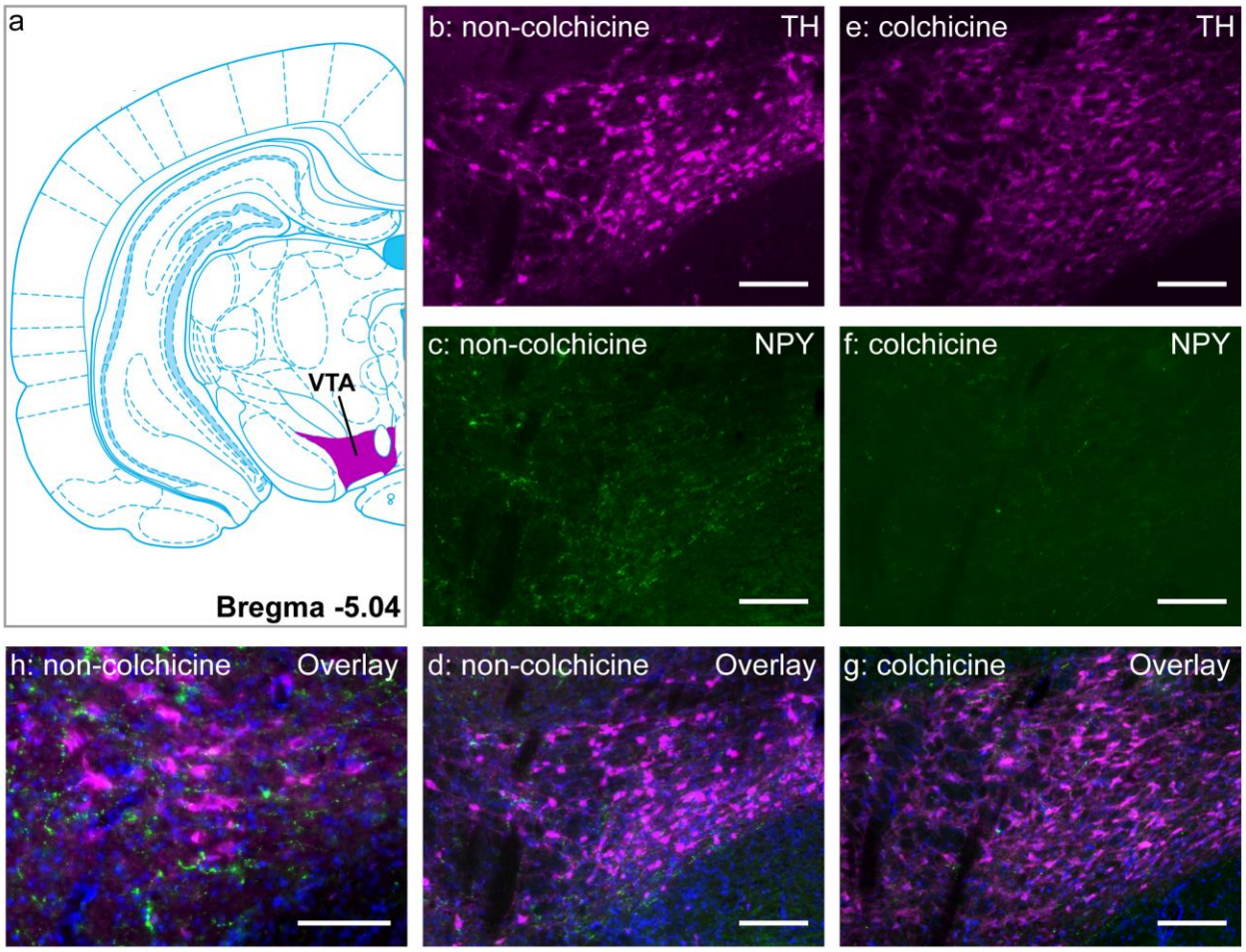

Figure 1. NPY-immunoreactive fibers, but not cell bodies, in the VTA. **a)** Drawing of a coronal atlas section at Bregma -5.04 mm indicating the representative VTA area as shown in further pictures. Atlas figure adapted from Paxinos and Watson (2007). **b, c, d)** Tyrosine hydroxylase (TH) staining, NPY staining, and an overlay with nuclear staining (Hoechst) staining in non-treated rats. **e, f, g)** TH, NPY and an overlay staining with nuclear staining in colchicine-treated rats. **h)** Overlay image showing TH, NPY, and Hoechst staining in slices of non-treated rats at 20X magnification. b-g at 5X magnification, scale bar = 100µm; h, scale bar = 150 µm; TH = magenta, NPY = green, Hoechst = blue.

Modulation of *Npy* expression by physiologic state

Next, we used RT-qPCR, a sensitive method that allows the measurement of very low mRNA copy numbers (Bustin, 2000), to exclude that VTA neurons express *Npy*. In *ad libitum*-fed normal weight male rats, *Npy* expression in VTA punches was practically negligible compared to *Npy* expression in the Arc, but not completely absent (Figure 3a). NPY levels vary with physiological state in certain brain regions. For example, a 24-hour fast increases *Npy* expression in the Arc of the hypothalamus (Hahn et al., 1998; Marks et al., 1992). We therefore determined if 24 hours fasting induces *Npy* expression locally in the VTA. See Figure 3B for the experimental setup and Figure 3c for the punch areas. In accordance with previous studies (Hahn et al., 1998; Marks et al., 1992), Arc *Npy* expression was increased by

approximately 40% after a 24 hours fast (Figure 3a; Two-way ANOVA interaction: $F_{1,22} = 317.9$, $p < .0001$; *post hoc* Arc ad lib *vs.* fasting, $p = .0007$). In contrast, a 24-hour fast did not modulate VTA *Npy* expression, which remained practically negligible (Figure 3a; *post hoc* VTA ad lib *vs.* fasting, $p > 0.05$). We also measured expression of two NPY receptors, *Npy1r* and *Npy5r*, in the VTA. Both receptors were expressed in the VTA, but not regulated by a 24-hour fast (data not shown). Together with our neuroanatomical data, these observations confirm that the origin of endogenous VTA NPY comes predominantly, if not completely, from an afferent projection to the VTA.

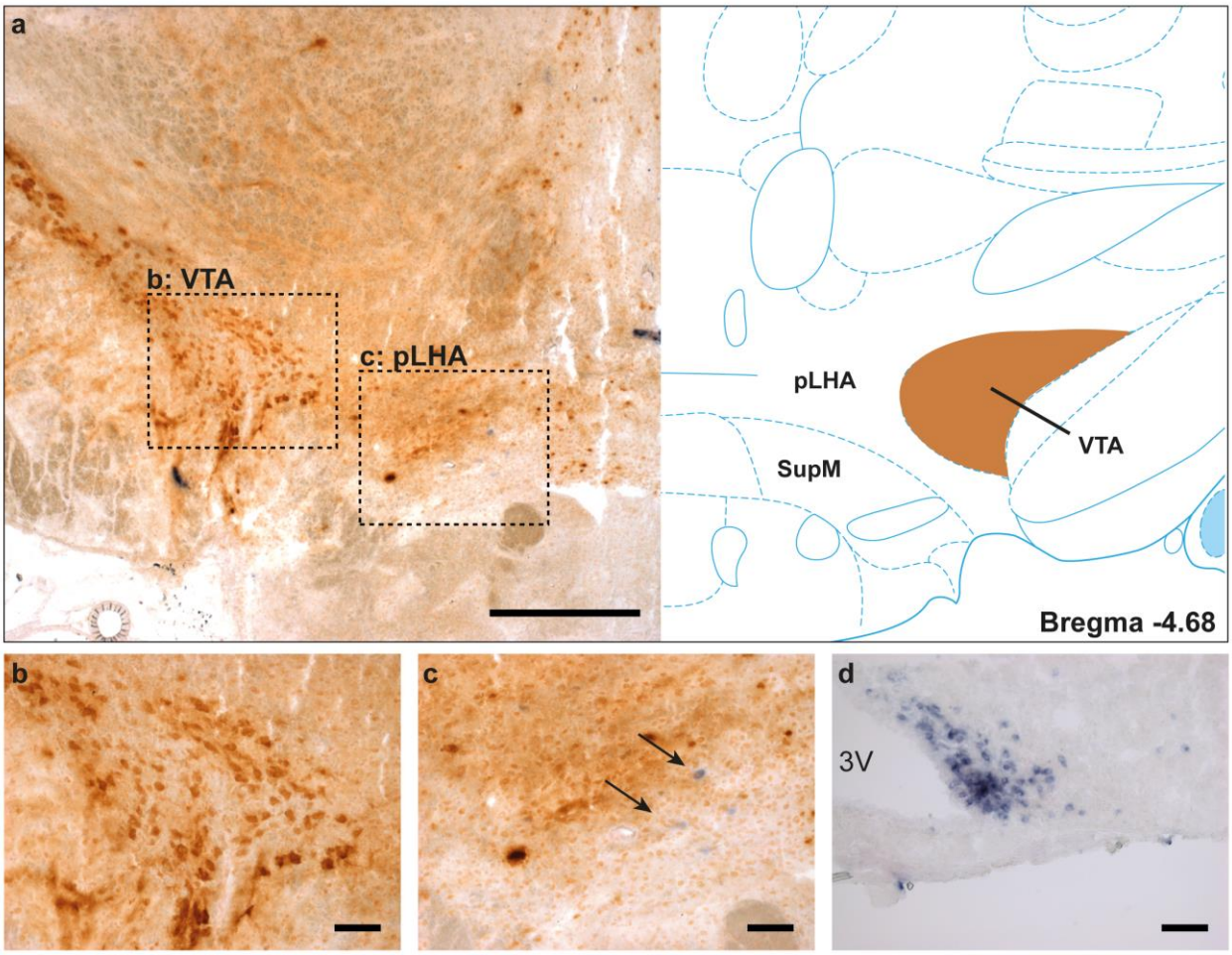

Figure 2. *Npy*-expressing cell bodies in the posterior lateral hypothalamic area, but not in the VTA. **a, left)** A coronal VTA section at Bregma -4.68 mm stained for *Npy* (blue) by *in situ* hybridization and tyrosine hydroxylase (TH; brown) immunocytochemistry, and **(a, right)** drawing of a coronal atlas section to indicate the VTA, posterior lateral hypothalamic area (pLHA), and the medial supramammillary nucleus (SupM). Atlas figure adapted from Paxinos and Watson (2007). **b)** Inset of the VTA area showing TH-positive cell bodies, but absence of *Npy*-positive cell bodies. **c)** Inset of the pLHA/SupM showing *Npy*-positive cell bodies, indicated by arrows. **d)** A coronal Arc section showing *Npy*-positive cell bodies. a, scale bar = 500µm; b-d, scale bar = 100 µm.

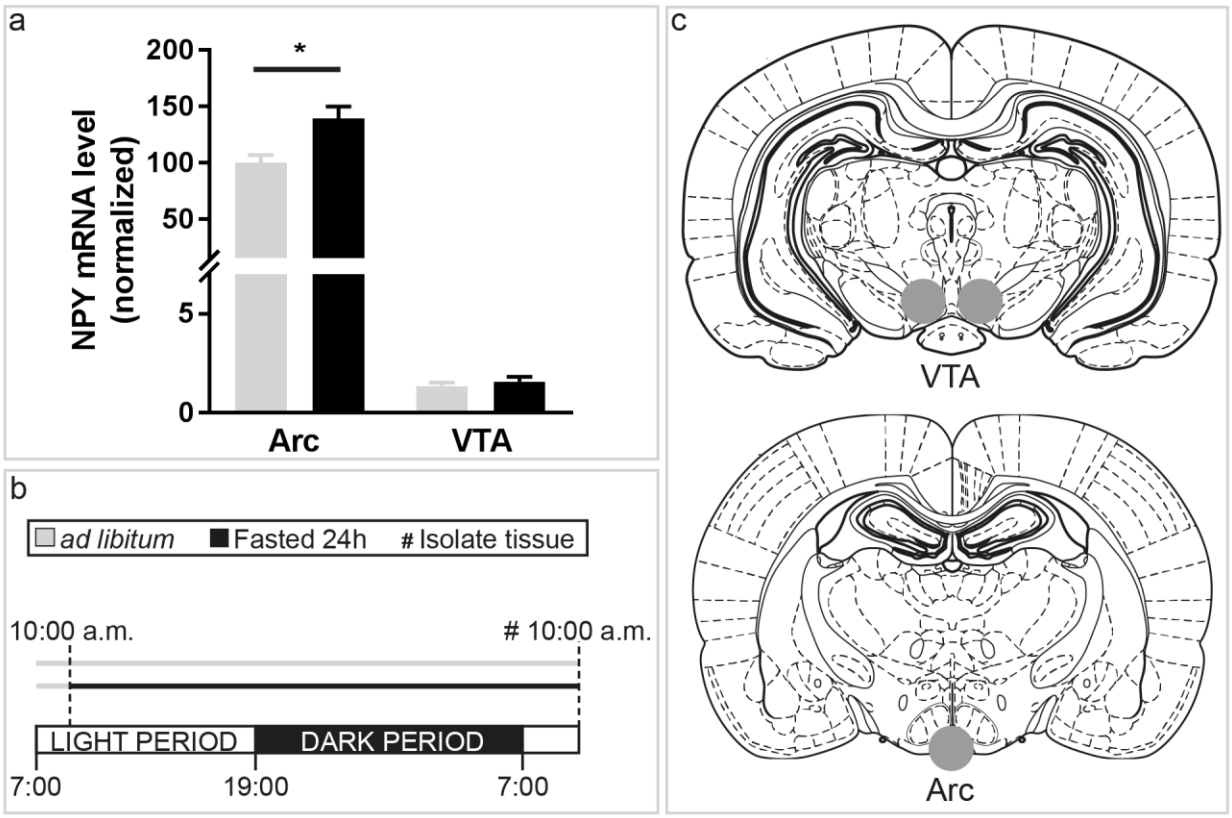

Figure 3. A 24-hour fast increases *Npy* expression in the Arc, but does not induce *Npy* expression in the VTA. a) *Npy* expression in the Arc and VTA at the beginning of the light period, normalized to three reference genes and expressed as a percentage of Arc *ad libitum* levels. *Npy* expression in the Arc was modulated by a 24-hour fast (*post hoc;* * = $p < .001$). VTA *Npy* expression was barely detectable compared to Arc levels, and not modulated by a 24-hour fast (*post hoc*; $p > 0.05$). **b)** Schematic overview of the experimental setup and timeline. Rats were fasted for 24 hours or fed *ad libitum* before sacrifice at the beginning of the light period. **c)** Coronal rat brain drawing indicating the punch areas for the respective regions. Atlas figures adapted from Paxinos and Watson (2007). N = 6/7 per group.

Identification of NPY-immunoreactive afferents to the VTA

To study the origin of NPY afferents to the VTA, we infused the retrograde tracer CTB into the VTA, followed by infusion of colchicine prior to sacrifice to enhance visualization of NPY (de Quidt & Emson, 1986a). Six rats showed CTB infusions confined to the VTA region (Figure 4a-d). In these animals, whole-brain serial sections showed CTB-labelling throughout the brain (Figure 5) in a pattern consistent with previously reported VTA afferents (Geisler & Zahm, 2005; Yetnikoff et al., 2014). Throughout the brain, several regions showed both NPY-immunoreactive neurons and CTB-containing neurons. We included all regions known to contain NPY neurons, to project to the VTA and to be involved in motivational or reward-related behavior (see Table 3).

In all six rats, the Arc of the hypothalamus contained neurons that were double-stained with NPY and CTB (Figure 6a-b). Over all animals, mean estimated total numbers of 293 ± 42 CTB-positive neurons and 64 ± 20 CTB/NPY-positive were calculated ipsilaterally to the infusion site. Contralaterally, mean estimated total numbers of 224 ± 40 CTB-positive and 57 ± 21 CTB/NPY-positive neurons were calculated. Of the CTB-positive neurons, mean percentages of 19.8 ± 5.0 % and 21.9 ± 5.8 % co-localized with NPY ipsilaterally and contralaterally, respectively, throughout the entire rostro-caudal extent of the Arc. Figure 6C shows the Arc NPY region of interest schematically.

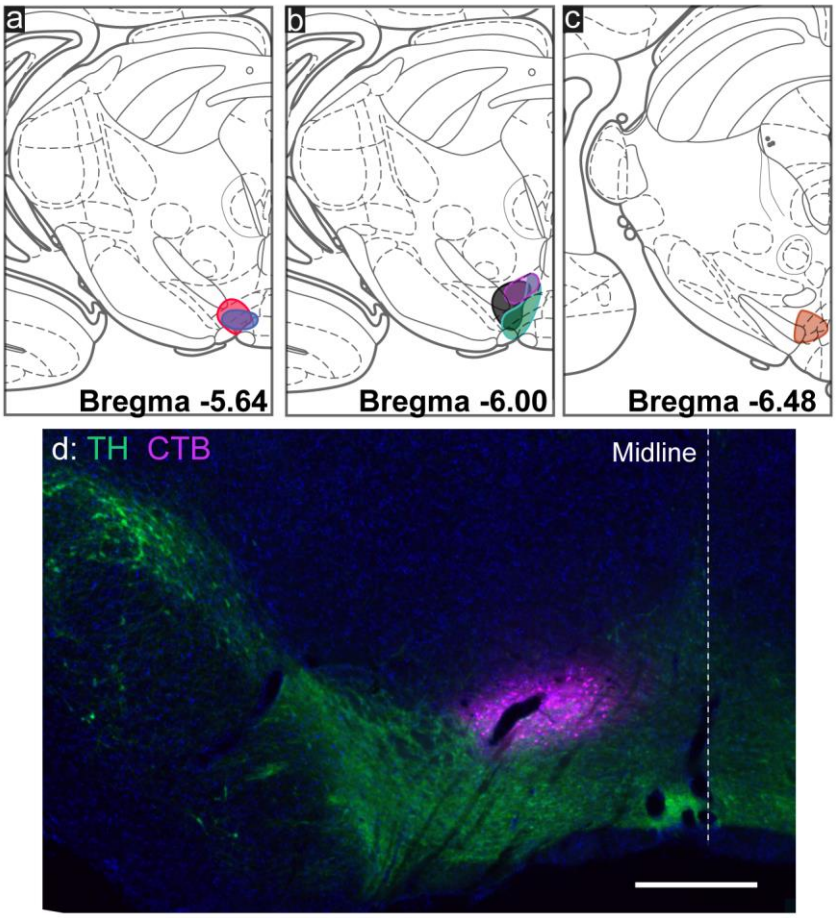

Figure 4. CTB infusion sites. a - c) Overview of the 6 experimental animals with the retrograde tracer CTB confined to the VTA and used for the analysis. The region with the largest area in the coronal plane is shown at the respective Bregma level. **d)** Example of CTB infusion site (magenta area in b), showing tyrosine hydroxylase (TH, green), CTB (magenta) and Hoechst (blue). Atlas figures adapted from the rat brain atlas (Paxinos & Watson, 2007). Scale bar = 500 µm.

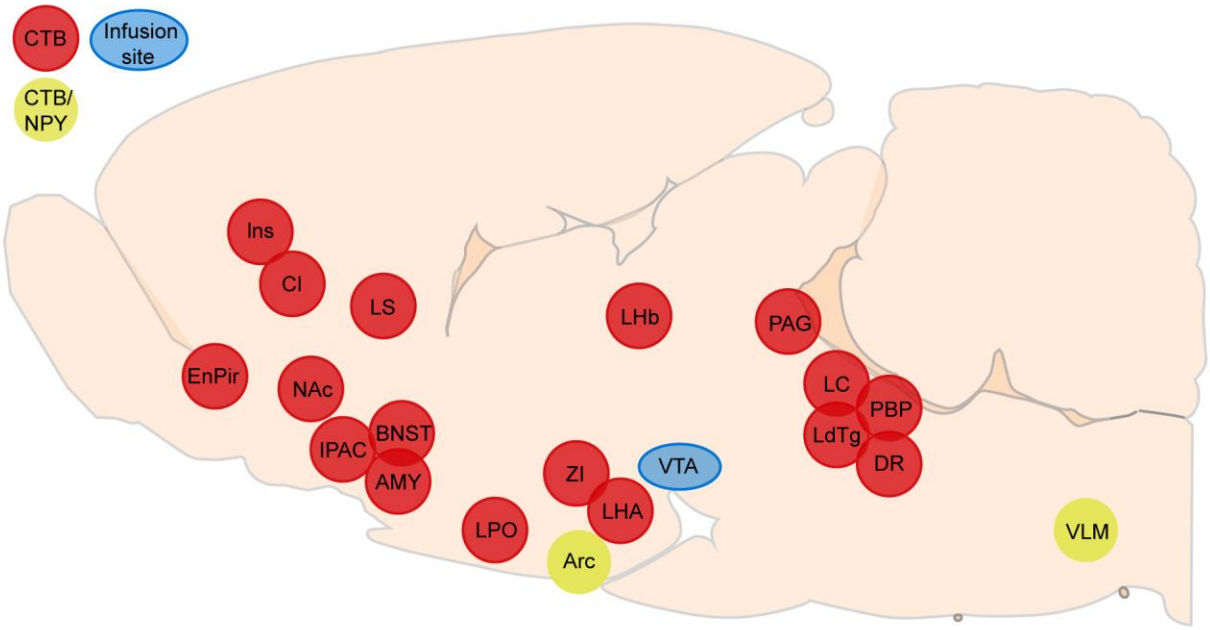

Figure 5. Schematic overview of identified VTA afferents using CTB. Schematic sagittal rat brain drawing showing a selection of the brain regions containing CTB neurons (red areas) following CTB infusion into the VTA (blue). The Arc of the hypothalamus and the ventrolateral medulla are the only regions showing CTB/NPY co-localization (areas indicated in yellow). Not all projections are shown for clarity. Atlas figure adapted from the rat brain atlas (Paxinos & Watson, 2007). Arc = arcuate nucleus of the hypothalamus, AMY = amygdala (all amygdala regions), BNST = bed nucleus of the stria terminalis, Cl = claustrum, DR = dorsal raphe, EnPir = Endopiriform nucleus and piriform cortex, Ins = insular cortex, IPAC = Interstitial nucleus of the posterior limb of the anterior commissure, LdTg = laterodorsal tegmental nucleus, LHA = lateral hypothalamic area, LHb = lateral habenula, LC = locus coeruleus, LPO = lateral preoptic area, LS = lateral septum, NAc = nucleus accumbens, PAG = periaqueductal grey, PBP = lateral and medial parabrachial nucleus, VLM = ventrolateral medulla, VTA = ventral tegmental area, ZI = zona incerta.

Based on known VTA projections (Geisler & Zahm, 2005; Mejias-Aponte, Drouin, & Aston-Jones, 2009) and brainstem NPY expression (Chronwall et al., 1985; de Quidt & Emson, 1986a; Everitt et al., 1984; Yamazoe et al., 1985), we also expected co-localization of CTB and NPY in several brainstem structures and thus analyzed the brainstem of four CTB-infused brains (from Figures 4a-c; magenta, green, black and orange color-coded animals were analyzed). The ventrolateral medulla showed co-localization of CTB and NPY that was limited to a region from Bregma -12.12 till -15.00 mm (Figures 7a-c). Mean estimated total numbers of 193 ± 64 CTB-positive neurons and 65 ± 23 CTB/NPY-positive neurons were calculated ipsilaterally. Contralaterally, mean estimated total numbers of 230 ± 84 CTB-positive neurons and 28 ± 11 CTB-NPY-positive neurons were calculated. Of the CTB-positive neurons, a mean percentage of 33.8 ± 8.2 % and 16.0 ± 6.2 % co-localized with NPY ipsilaterally and contralaterally

respectively, in the ventrolateral medulla. Thus, the Arc as well as a part of the ventrolateral medulla of the brainstem contain NPY-immunoreactive afferents projecting to the VTA in normal-weight male Wistar rats.

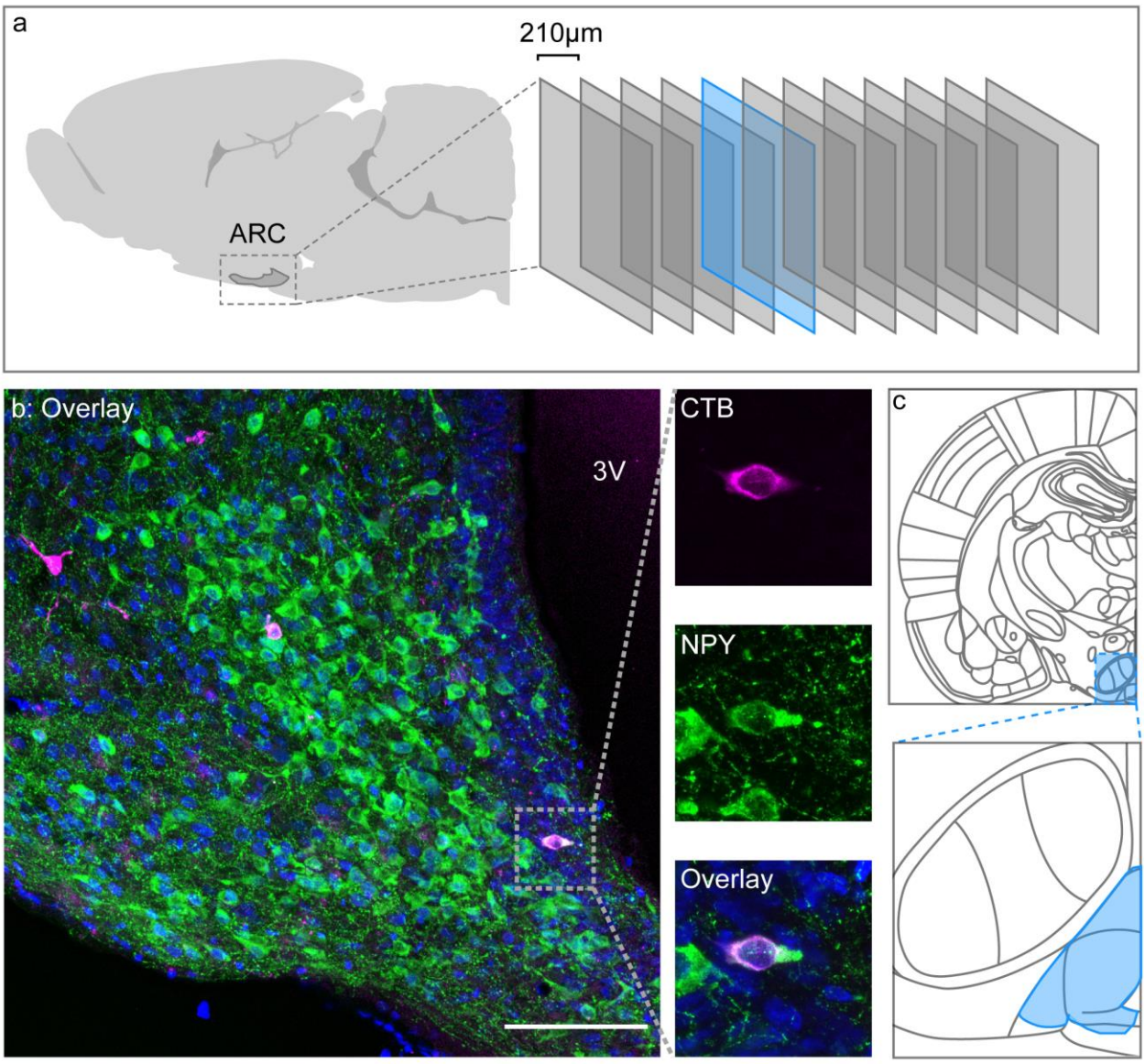

Figure 6. Arc NPY-immunoreactive cell bodies project to the VTA. a) Sagittal rat brain drawing showing the location of the Arc and the slice shown in (b). **b)** Randomly selected confocal fluorescent image series of a coronal Arc section showing CTB (magenta), NPY (green), Hoechst (blue), and co-localization of CTB and NPY (white). The inset is made at 63X magnification. **c)** Coronal image showing the approximate region of interest for CTB cell counts in the NPY area. Atlas figures adapted from the rat brain atlas (Paxinos & Watson, 2007). Scale bar = 100 µm, 3V = third ventricle.

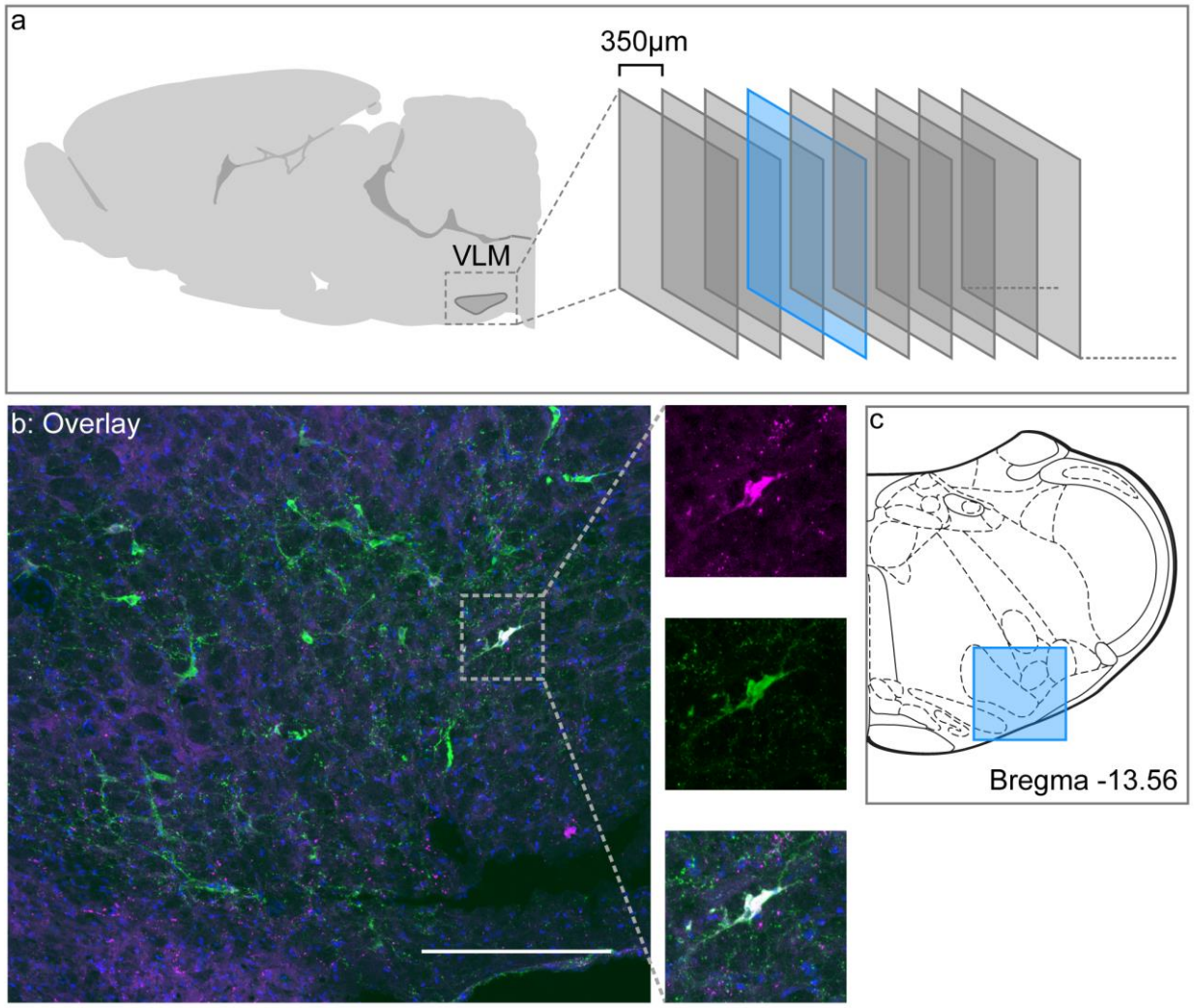

Figure 7. Ventrolateral medullar NPY-immunoreactive cell bodies project to the VTA. a) Sagittal rat brain drawing showing the location of the ventrolateral medullar area and the slice shown in (b). **b)** Randomly selected confocal fluorescent image series of a coronal section showing CTB (magenta), NPY (green), Hoechst (blue), and co-localization of CTB and NPY (white) and a zoom on a co-localizing cell body (magnification 20X). **c)** Atlas figure showing the location of the image in (b). Atlas figures are adapted from the rat brain atlas (Paxinos & Watson, 2007). Scale bar = 250 µm.

Table 3. Overview of NPY-immunoreactive afferent projections to the VTA. Regions were selected based on the current literature showing both a VTA afferent projection and NPY soma by immunocytochemistry.

VTA afferent containing NPY cell bodies	VTA afferent	NPY soma	Co-localization	Conclusion
Telencephalon				
Claustrum	Yes	Yes	No	Non-NPY projection
Endopiriform n. + piriform cortex†	Yes	Yes	No	Non-NPY projection
Insular cortex	Yes	Yes	No	Non-NPY projection
Nucleus accumbens (core and shell)	Yes	Yes	No	Non-NPY projection
Bed nucleus of the stria terminalis	Yes	Yes	No	Non-NPY projection
IPAC‡	Yes	Yes	No	Non-NPY projection
Medial preoptic nucleus	Yes	Yes	No	Non-NPY projection
Ventral Pallidum	Yes	Yes	No	Non-NPY projection
Amygdala§	Yes	Yes	No	Non-NPY projection
Lateral septum	Yes	Yes	No	Non-NPY projection
Diagonal band of Broca	Yes	No	No	Non-NPY projection
Lateral preoptic area	Yes	Yes	No	Non-NPY projection
Cingulate cortex	Yes	Yes	No	Non-NPY projection
Diencephalon				
Arcuate nucleus of the hypothalamus	**Yes**	**Yes**	**Yes**	**NPY projection**
Anterior hypothalamus	Yes	Yes	No	Non-NPY projection
Hypothalamic paraventricular nucleus	Yes	No	No	Non-NPY projection
Ventromedial hypothalamic nucleus	Yes	No	No	Non-NPY projection
Zona incerta	Yes	No	No	Non-NPY projection
Perifornical lateral hypothalamic area	Yes	No	No	Non-NPY projection
Dorsal hypothalamus	Yes	No	No	Non-NPY projection
Posterior lateral hypothalamus	Yes	Yes	No	Non-NPY projection
Mesencephalon				
Periaqueductal gray¶	Yes	Yes	No	Non-NPY projection
Met- and Myelencephalon				
Locus coeruleus	Yes	Yes	No	Non-NPY projection
Laterodorsal tegmental nucleus	Yes	No	No	Non-NPY projection
Dorsal Raphe	Yes	No	No	Non-NPY projection
(Lateral) of Central Gray	Yes	Yes	No	Non-NPY projection
Lateral parabrachial nucleus	Yes	No	No	Non-NPY projection
Medial parabrachial nucleus	Yes	No	No	Non-NPY projection
Ventrolateral medulla	**Yes**	**Yes**	**Yes**	**NPY projection**

† As fluorescent immunocytochemistry does not allow the separation of the endopiriform nucleus and piriform cortex, these structures were analyzed together. ‡ IPAC = Interstitial nucleus of the posterior limb of the anterior commissure. § As no co-localization of NPY and CTB was found throughout all amygdala regions, these regions were analyzed together. ¶ The periaqueductal grey for the magenta case in Figure 4 contained 2 CTB/NPY positive cell bodies, out of >15 CTB-positive cell bodies per brain slice containing the periaqueductal grey.

Identification of POMC-immunoreactive Arc afferents to the VTA

We next investigated the identity of CTB-positive neurons in the Arc that did not express NPY. POMC-expressing neurons represent another major population of neurons in the Arc, which are separate from the NPY population, and also project to the VTA (Hahn et al., 1998; Pandit et al., 2015). We confirmed that Arc POMC-immunoreactive neurons project to the VTA, and quantified the Arc POMC projection in the same brains used for NPY tracing (Figures 8a-c). Mean estimated total numbers of 592 ± 84 CTB positive neurons and 689 ± 174 CTB/NPY-positive neurons were calculated ipsilaterally to the infusion site. Contralaterally, mean estimated total numbers of 134 ± 16 CTB and 142 ± 17 CTB/NPY-positive neurons were calculated. The mean percentage of the CTB-positive neurons co-localizing with POMC was 21.7 ± 1.7 % ipsilaterally, and 28.7 ± 4.2 % contralaterally. Figure 8d shows the Arc POMC region of interest schematically.

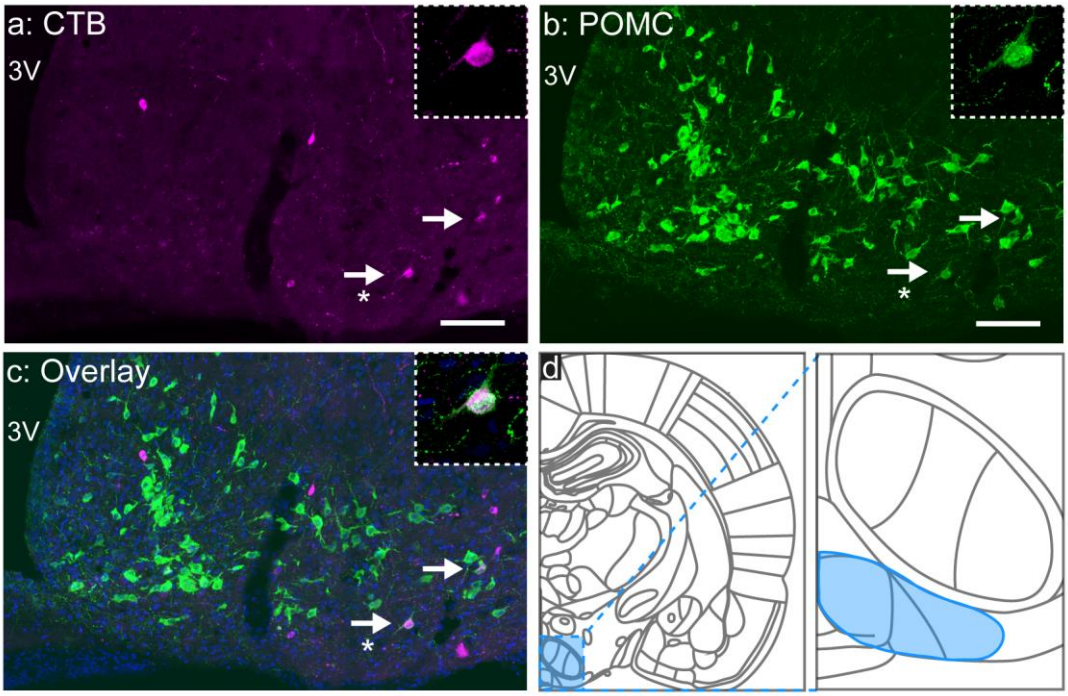

Figure 8. POMC neurons in the Arc project to the VTA. Confocal fluorescent image series at 20X magnification showing **a)** CTB (magenta), **b)** POMC (green), and **c)** an overlay with Hoechst (blue) in a coronal section of the Arc. **d)** Coronal drawing showing the approximate region of interest for CTB cell counts in the POMC area. Atlas figures are adapted from the rat brain atlas (Paxinos & Watson, 2007). Arrows indicate co-localization. Scale bar = 100 µm. * = insets at 63X. 3V = 3rd ventricle.

Discussion

In the present study, we have characterized NPY-immunoreactive afferents projecting to the VTA. Using immunocytochemistry, we observed NPY-immunoreactive fibers, but not NPY-expressing cell bodies, in the VTA. NPY fibers in the VTA were not visible following treatment with colchicine, which arrests neuronal peptide transport. As colchicine treatment also did not lead to visualization of NPY cell bodies in the VTA and no *Npy*-expressing cell bodies were found using *in situ* hybridization, this indicates that the NPY-immunoreactive fibers come from afferent projections to the VTA. Accordingly, following infusion of the retrograde tracer CTB in the VTA, we identified cellular co-localization of CTB and NPY in the Arc of the hypothalamus and in the ventrolateral medulla of the brainstem. We did not observe co-localization in any other brain region. To investigate if an altered metabolic state could induce *Npy* expression within the VTA, we also measured *Npy* expression following a 24-hour fast using the sensitive RT-qPCR method. However, the 24-hour fast, which was sufficient to increase *Npy* expression in the Arc, did not modulate the barely detectable levels of *Npy* expression in the VTA. Collectively, our data indicate that the Arc of the hypothalamus and the ventrolateral medulla of the brainstem are the only brain regions that contain NPY-immunoreactive afferents that project to the VTA under normal physiological circumstances.

To date, detection of NPY-immunoreactive cell bodies in the VTA has produced inconsistent results, likely driven by variation in experimental methods, such as differences in species or colchicine treatment dose and duration (Chronwall et al., 1985; de Quidt & Emson, 1986a; Everitt et al., 1984). Similar to the study of de Quidt and Emson (1986a), we did not observe NPY- or *Npy*-expressing cell bodies using immunocytochemistry or *in situ* hybridization, respectively. However, using RT-qPCR, a much more sensitive technique compared to *in situ* hybridization, we detected practically negligible *Npy* expression in the VTA compared to the Arc. As we identified *Npy*-expressing cell bodies in the posterior lateral hypothalamic area/medial supramammillary nucleus, located adjacent to the VTA (Figure 2a), it is likely that the very low number of *Npy* mRNA copies observed by RT-qPCR result from accidental inclusion of *Npy*-expressing cell bodies in the posterior lateral hypothalamic area/medial supramammillary nucleus in our punched VTA samples.

Despite the inconsistency in observing NPY-immunoreactive cell bodies, our study as well as all previous studies, consistently observed NPY-immunoreactive fibers in the VTA. In accordance with the presence of Agouti-related protein (AgRP)-immunoreactive fibers in the VTA (Broberger, Johansen, et al., 1998; Dietrich et al., 2012), we found that a subset of Arc NPY-immunoreactive neurons project to the VTA. AgRP is found exclusively in the Arc, where it co-localizes almost entirely with NPY neurons (Broberger, Johansen, et al., 1998; Hahn et al., 1998). Although the Arc—>VTA projection is considered to be relatively small compared to other VTA afferents (Geisler & Zahm, 2005; Watabe-Uchida et al., 2012), general activation of

Arc NPY/AgRP neurons using a chemogenetic approach increases motivation to obtain food pellets, suggesting a behaviorally functional and important role for this projection in motivational and behavioral aspects of feeding behavior (Krashes, Shah, Koda, & Lowell, 2013).

We also confirm that Arc POMC neurons project to the VTA (Pandit et al., 2015). Despite a comparable percentage of VTA-projecting neurons being NPY and POMC (20 - 30%), it has to be noted that the absolute number of Arc CTB/POMC neurons is larger than the number of Arc CTB/NPY neurons. We believe that this difference is likely attributable to the larger POMC area in the Arc that was used for the cell counts due to the lack of visible anatomic markers for the Arc (see Materials and Methods, and Figures 6 and 8). NPY and POMC neurons are separate populations in the Arc with opposing effects on feeding behavior and energy expenditure (Aponte, Atasoy, & Sternson, 2011; Hahn et al., 1998). Future studies, utilizing chemogenetic or optogenetic manipulation of these VTA-projecting Arc NPY and POMC neuronal populations, will provide valuable insight into the role of these neurons in motivational and behavioral aspects of feeding behavior.

In addition to the NPY-immunoreactive Arc—>VTA projection, we also observed co-localization of CTB and NPY in the ventrolateral medulla of the brainstem. This VTA afferent projection has previously been demonstrated using the CTB tracing approach (Geisler & Zahm, 2005), and several regions in the ventrolateral medulla contain NPY neurons, including the A1 and C1 catecholaminergic cells groups (Everitt et al., 1984; Sawchenko et al., 1985). The population co-localizing neurons that we found is located similarly to the A1 and C1 regions. In addition, NPY neurons in the ventrolateral medulla almost completely co-localize with markers for catecholaminergic neurons (Everitt et al., 1984; Harfstrand et al., 1987; Sawchenko et al., 1985; Tseng, Lin, Wang, & Tung, 1993) and ventrolateral medulla catecholaminergic projections to the VTA were observed in male Sprague Dawley rats (Mejias-Aponte et al., 2009). Together, this might indicate that the NPYergic brainstem—>VTA projection is (partially) catecholaminergic. Several studies indicate a role for catecholaminergic/NPY neurons in this area in the regulation of feeding and energy homeostasis. For example, specifically catecholaminergic/NPY neurons in the caudoventrolateral medullar area are necessary for glucoprivic feeding (A. J. Li et al., 2009). Also, *Npy* overexpression in catecholaminergic brainstem neurons alters body composition independent of changes in food intake (Ruohonen et al., 2008; Ruohonen, Vahatalo, & Savontaus, 2012; L. Zhang et al., 2014). Though catecholaminergic/NPY neurons in the A1/C1 regions project to the hypothalamus (Sawchenko et al., 1985), a role for their possible connection with the VTA in regulating the above-mentioned processes cannot be excluded, and despite the relatively small size of the VTA afferent projection, it may have a substantial impact on energy homeostasis. However, additional anatomical studies will have to determine whether the NPYergic VTA projecting neurons are indeed catecholaminergic.

Mechanistic studies can target the VTA-projecting NPY-expressing neurons in the ventrolateral medulla to determine their role in feeding-related motivational behaviors.

Brain area-specific NPY expression can fluctuate during increased motivation as well as hyperphagia. For example, both Arc *Npy* expression and the number of Arc NPY neurons increases during a 24-hour fast (see Figure 3B and, e.g., [Hahn et al., 1998]), and hindbrain A1/C1 *Npy* expression increases during glucoprivation (A. J. Li & Ritter, 2004). Furthermore, NPY-immunoreactive cell bodies are not commonly observed in the rat dorsomedial hypothalamus during adulthood, yet they become apparent in lactating females as well as in diet-induced obese rodents (Kesterson, Huszar, Lynch, Simerly, & Cone, 1997; C. Li, Chen, & Smith, 1998a). In this study, we demonstrate that a 24-hour fast was not associated with increased local VTA *Npy* expression. We cannot, however, exclude that the number and/or identity of NPY-immunoreactive VTA afferents is different between sexes or during conditions with altered physiological needs, such as pregnancy and diet-induced obesity, compared to the standard physiological condition assessed in this study. In addition, infusion of colchicine in the lateral ventricle may not lead to a uniform increase in immunoreactivity in the brain, particularly in the hindbrain areas, and our tracer injection did not encompass the entire VTA, which may lead to an underestimation of the number of co-localized neurons. Lastly, the CTB tracer is not unsusceptible to uptake by fibers of passage, which could lead to the identification of a non-existent NPY-containing VTA afferent (S. Chen & Aston-Jones, 1995; Ericson & Blomqvist, 1988; Luppi, Fort, & Jouvet, 1990). However, the two projections we have determined to be partially NPYergic have been described in a tracing study employing retrograde viral tracers specifically targeted to VTA dopaminergic neurons by using the Cre-Lox system (Watabe-Uchida et al., 2012). As uptake by fibers of passage is highly unlikely with this technique, we therefore believe that the assessment of NPY afferents in our study is accurate.

We demonstrate that both the Arc and a part of the ventrolateral medulla of the brainstem contain NPY-immunoreactive afferents projecting to the VTA under normal physiological circumstances in normal-weight male Wistar rats. Therefore, these brain regions link the NPY circuitry to VTA-driven changes in motivational behavior. Our study is the first to systematically investigate the origin of VTA afferent projections using neuroanatomical tracing methods. The next step will be to establish how these neuronal populations drive VTA-driven motivational behavior and whether the function of these populations is dysregulated during altered physiological states, including obesity.

Acknowledgements

We thank Joop van Heerikhuizen and Joris Coppens from The Netherlands Institute for Neuroscience for imaging expertise and Ewout Foppen for providing the brain samples for the RT-qPCR experiment. This work was supported by an AMC PhD scholarship grant awarded to MCRG by the AMC Executive Board and by the Netherlands Organization of Scientific Research (NWO-VICI grant 016.160.617).

Table 2. Antibodies used in this study.

Antibody (dilution)	Immunizing agent	Manufacturer/Cat#/RRID/Clonality	Reference
Rabbit anti-NPY (1:1,000)	Full porcine NPY-peptide conjugated to thyroglobulin with glutaraldehyde: YPSKPDNPGEDAPAEDLARYYSALR HYINLITRQRY-NH2	Netherlands Institute for Neuroscience/n.a./RRID: AB_2753189/ polyclonal	*
Rabbit anti-POMC (1:1,000)	N-terminal 26 amino acids of porcine POMC: WCLESSQCQDLSTESNLLACIRCAC KP	Phoenix Pharmaceuticals/ #H-029-030/RRID: AB_2307442/polyclonal	(Wittmann et al., 2017)
Mouse anti-TH (1:1,000)	Tyrosine hydroxylase purified from PC12 cells	EMD Millipore Corporation/ #MAB318/RRID: AB_2201528/ monoclonal	(H. L. Wang & Morales, 2008)
Rabbit-anti-TH (1:1,000)	SDS-denatured rat tyrosine hydroxylase purified from pheochromocytoma	Sigma-Aldrich/#T8700/n.a./ polyclonal	n.a.
Biotinylated goat anti-mouse IgG (H+L) (1:400)	Mouse IgG	Vector Laboratories/ BA9200/RRID: AB_2336171/polyclonal	n.a.
Biotinylated goat anti-rabbit IgG (H + L) (1:400)	Rabbit IgG	Vector Laboratories/ BA1000/RRID: AB_2313606/polyclonal	n.a.
Alexa Fluor-488 donkey anti-rabbit IgG (H+L) (1:500)	Rabbit IgG	Invitrogen/A21206/RRID: AB_2535792/polyclonal	n.a.

n.a. = not applicable, *(Buijs, 1989; Goldstone et al., 2002; van der Beek et al., 1992; van Wamelen et al., 2013)